TECTONIC SETTING AND UPLIFT ANALYSIS OF THE PANGANI RIFT BASIN IN NORTHERN TANZANIA USING APATITE FISSION TRACK THERMOCHRONOLOGY

EI Mbede
Department of Geology, University of Dar es Salaam,
P. O. Box 35052, Dar es Salaam, Tanzania

ABSTRACT

Thirty four new Apatite Fission Track (AFT) ages and 32 track length distributions from samples of basement rocks flanking the Pangani rift, East African Rift System (EARS) are presented, in an attempt to elucidate the uplift and erosion of the rift flanks. The ages fall in the range of 207 ±15 to 48±4 Ma, spanning from Early Jurassic to Early Tertiary. These ages are much younger than the last thermal event in the Mozambique belt that form the basement complex and are interpreted to represent the most recent tectonic events. Track length (TL) distributions suggest that uplift and erosion of the rift flanks are related to three different tectonic events, which are also recorded by the sedimentary units within the adjacent coastal basins. These include the Triassic/Early Jurassic, Late Cretaceous and Early Tertiary tectonic events. Erosion and isostatic rebound have modified the tectonically induced topographic patterns and the highly elevated plateaus flanking the Pangani rift represent an erosional surface referred to as the "Gondwana surface" of eastern and central Africa. The present AFT data suggest that initial exhumation of the "Gondwana surface" from temperatures above 110°C to temperatures less than 60°C, in this area, took place during Early Jurassic times, but the final sub-aerial exposure of the surface did not take place until Early Tertiary.

INTRODUCTION

Of the three arms of the East African Rift System in the northern Tanzania divergence (Ebinger *et al.* 1996), the roughly N-S trending Natron-Manyara-Barangida rift; the NE trending Eyasi-Manonga-Wembere rift and the N to NW trending Pangani rift (Fig. 1), Pangani rift has been the least researched in recent years. Seismicity occurs throughout the Tanzania divergence but little activity is reported along the Pangani arm (Nyblade *et al.* 1997). However the youthful nature of the Pangani scarps and the freshness of faults and fracture systems, give evidence of recent movements. The faceted Pangani rift scarps

emerges south-eastward of mount Kilimanjaro traversing the Pare and Usambara mountains before dying out into the Mesozoic basin of coastal Tanzania. Basement rocks flanking the Pangani rift are made up of mainly granulites and granulitic gneisses which have been subjected to recumbent folding and horizontal translation (Bagnall 1962, Bagnall *et al.* 1963). The rift floor is formed by complex mobilised migmatite series with the regional eastward dip which seem to have developed by metasomatic granitisation of rocks of the garanulite facies covered by a relatively thin layer of sediments.

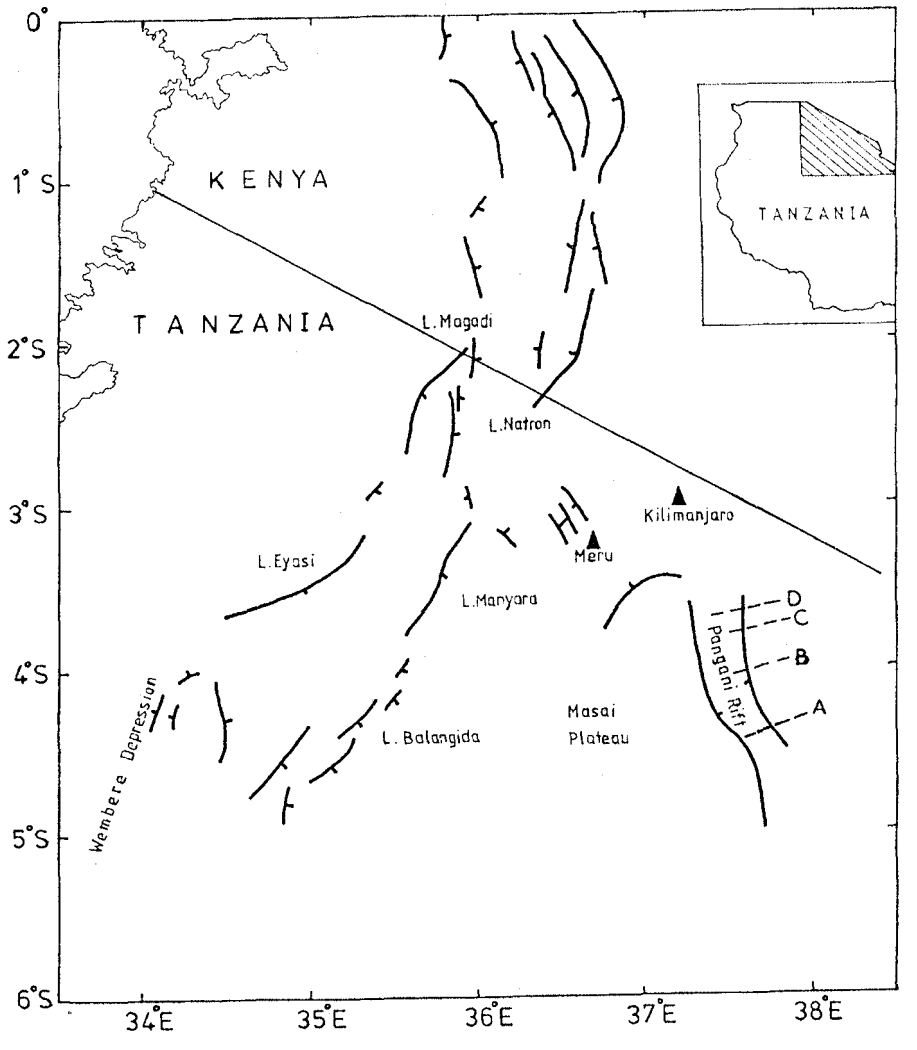

Fig. 1: Tectonic map of the northern Tanzania sector of the East African Rift System exemplifying the location of Pangani rift system, and the profiles sampled during this study. Profile locations are marked A, B, C and D representing the Usambara Mountain, the South Pare (Same scarp) mountain, the Kilomeni and the Usangi scarp profiles

The nature of the Pangani rift basin is not yet well understood because basement structures beneath the rift basin have not been well scrutinised. The eastern scarp is dissected into a number of faults by transfer faults that divide the North Pare from the South Pare and the Usambara mountain blocks rising to more than 2,000 m above the sea level (ASL) and tilted to the east towards the coastal basin. The three mountain blocks represent bounding faults of three separate sub-basins (Mbede 1999). Though the scarps of Pangani rift are highly faceted and elevated, showing the youthful nature of the rift, the age of faulting is less constrained. This study aimed at assessing the uplift and exhumation history of the Pangani rift flanks and correlating same with the various neotectonic events within this portion of the East African Rift System using the Apatite Fission Track dating method. Results suggest that the highly uplifted flanks of the Pangani rift are relict features of several phases of tectonic uplift events which were initiated during Early Jurassic, probably related to the last phase of Karoo faulting in eastern Africa. The final phase of significant tectonic uplift did not happen until Early Tertiary time.

Tectonic setting

The Pangani river basin is made up of the Pangani/Ruvu depression, which extends from the slopes of Mts. Meru and Kilimanjaro south and south-eastwards down stream till it joins the Indian ocean in Tanga. The basin encompasses the artificially created Nyumba ya Mungu dam and the basin shape is delineated in the Landsat imagery (Fig. 2). Within the study area, major structures, basin shape and basin geometry are clearly delineated in both the total magnetic field and derivative maps (Figs 3 and 4). Structurally both Figures 3 and 4 delineate a strong NNW trending structural grain throughout the study area clearly defining the basin geometry, the eastern and western boundaries of the basin and the major structural features. Within the basin, the amplitude of magnetic anomalies are lowest close to the eastern bounding fault, suggesting that the eastern bounding fault is the major boarder fault, i.e. sediment thicknesses increase in the direction of the bounding fault. The western bounding fault of the basin is more subdued and defines the eastern boundary of the Masai block.

Both the total magnetic field and the horizontal derivative maps suggest that Pangani rift basin is segmented into three sub-basins bound by major bounding fault systems, the North Pare border fault system, the South Pare boarder fault system and the Usambara mountain boarder fault system. The three sub-basins are separated by prominent NNE - SSW trending transfer faults. NNW-SSW trending ridges defined by basement high features stand out distinctly on the aeromagnetic maps within the basin and are also evident South of Nyumba ya Mungu dam in the Landsat image (Fig. 2). It is suggested that the NNW-SSW trend in this basin follows a zone of high mylonitisation that crosscut the main Gregory rift trend and the Mozambiquean belt trend in the region (McConnell 1972). Little can be inferred directly from the regions covered by volcanic rocks in the northern

part of the diagram where volcanic cones and associated flows are clearly delineated by the short wavelength and high amplitude anomalies. Besides, the low amplitude NNE-SSW to N-S striking structures are also prominent within the study area. These NNE-SSW to N-S striking structures and lithological contacts are clearly evident in the Precambrian sector of the Pare-Usambara mountains on the eastern part of the diagrams and within the Precambrian Masai block in the western part of the diagrams (Figs 3 and 4). The NNE-SSE and N-S trending structures, also isolated by the drainage pattern of the main tributaries of Pangani river (Fig. 2), are correlatable to the major regional trend of the Mozambique belt.

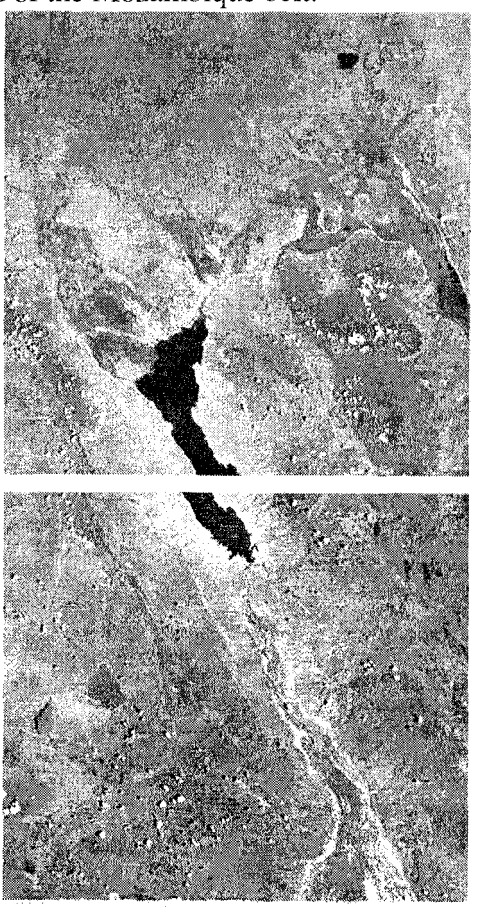

Fig. 2: Landsat image of the Pangani rift. Note that the water body at the mid of the image is the artificially created Nyumba ya Mungu dam whose southern tip is in close coincidence with the NNE trending transfer fault separating basins bound by the North Pare border fault system from that bound by the South Pare border fault system. Within the north Pare sub-basin, Landsat imagery suggests even lithology which indicates presence of much thicker sedimentary units compared to the other sub-basins. NW trending prominent ridges that represent basement highs are more evident south of Nyumba ya Mungu dam, these reflect thinning of sediment cover southwards

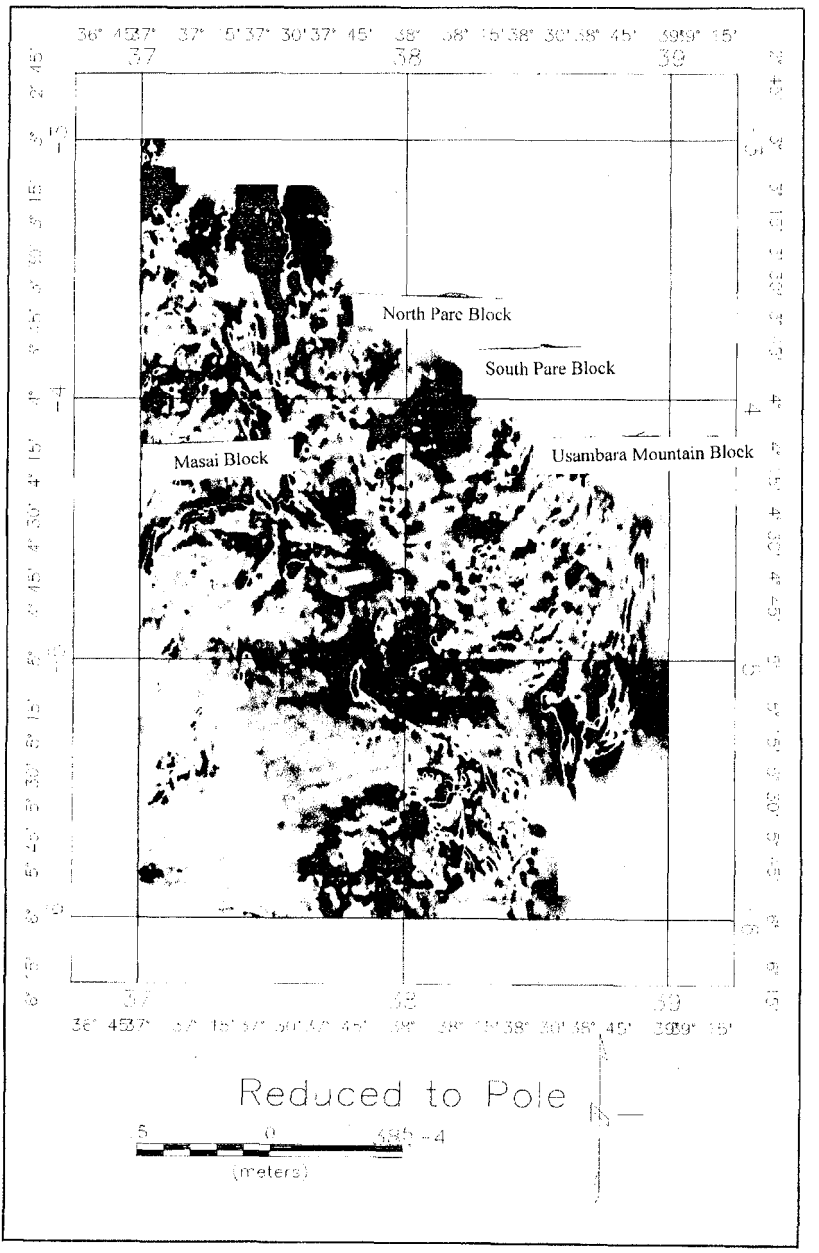

Fig. 3: Total magnetic map of Pangani basin, Tanzania

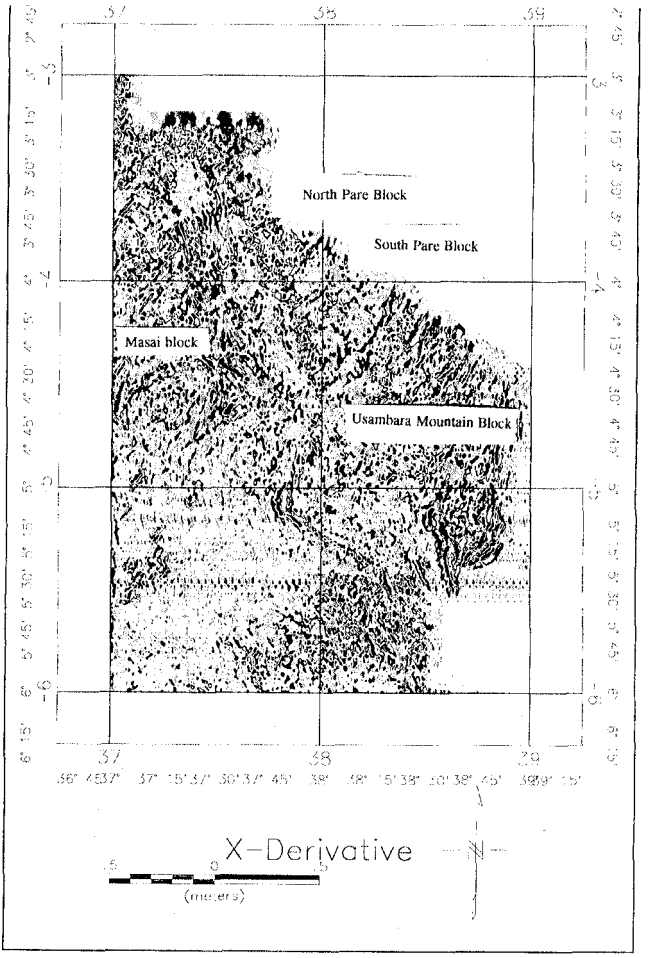

Fig. 4: Horizontal (X) derivative map of the Pangani basin, Tanzania

Thicknesses of sediments in the basin vary from place to place, clearly reflecting the three sub-basins defined above. On the overall the Pangani basin is a shallow basin, sediments are thick in the northern most sub-basin bound by the North Pare border fault system which encompasses the areas close to the slopes of Mts Meru and Kilimanjaro. Landsat image reveals even lithology within the basin that imply thick sediment deposits (Fig. 2). Sediments here are composed of mainly alluvial sediments, pyroclastics of the volcanic materials and lake beds summarised in the stratigraphic section (Fig. 5). South of Nyumba ya Mungu, the lithology within the basin becomes uneven, basement ridges become much more prominent suggesting thinning of the sedimentary cover. The southernmost basin bound by the Usambara mountain border fault system is defined by a more prominent magnetic basement covered by an unknown thickness of sedimentary strata. The basin is in most

parts covered by Quartenary lake beds of the Mbuga type of clays, reflecting the ephemeral lakes within Quartenary time in the variously subsiding components of the Pangani rift. Extent and thicknesses of the lake beds normally vary from place to place. The gypsiferous lake beds of Mkomazi-Makanya area are typical of those lake beds extending northwards from east of Mkomazi railway station. The exact thickness of lake beds in Mkomazi-Makanya area is not established. However, gypsum extraction has been done up to 3.68 m of lake beds still underlain by other sediments (Ilangali 1987).

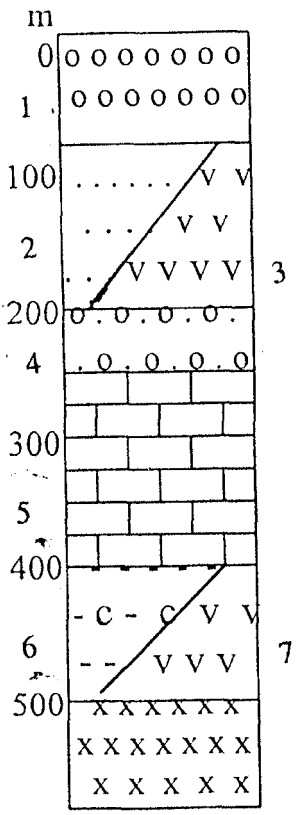

Fig. 5: Stratigraphic section of the north Pare sub-basin bound by the north Pare border fault system. 1. represents fan deposits made up of talus slope materials; 2. represents superficial deposits which constitute the alluvium, red soils, sand clays, gravels, boulders and locally calcareous material; 3. represents Kibo lavas that are boulders of basalt; 4. represents pyroclastic flows; 5. represents lacustrine deposits made up of calcareous agglomerate, limestones, clays and sands; 6. represents the Kibo lahar mud flows which show a debris nature of mud flows; 7. represents lava flows of scoria ash olivine basalt and trachytes; 8. represents the Precambrian cytstalline basement gneisses (Anon 1980)

METHODS

Aeromagnetic data processing

The aeromagnetic data used to generate both the total magnetic field and derivative maps (Figs 3 and 4) were collected by Geosurveys in 1977 and 1980 (Fairhead *et al.* 1988). Data collection was done using 1 km line spacing and 10 km tie line spacing on E-W flight lines throughout this region, excluding the area near the Kenya border where the flight lines were oriented N45W. Data were gridded at 1 km drape of topography, after removal of the main field (Fairhead *et al.* 1988). The horizontal derivative map of the data in the X (E-W) direction was computed from the total grid; map so generated, produce paired maximum or minimum values where maximum gradients exist, emphasising structures and magnetisation contrasts (Ebinger *et al.* 1996, Upcott *et al.* 1996).

Background on Apatite Fission track dating

Fission tracks are damage zones in the crystal lattice that have been formed as a result of spontaneous fission of ^{238}U. Upon fission, two positively charged high-energy fragments are formed and move away from each other, creating a single linear ionisation trail. All tracks are of the same size when formed, between 15 - 20 μm long and 25 - 50 Å wide, depending on the crystal density. Fission tracks become progressively shorter during thermal annealing; the rate of annealing increases non-linearly with temperature. Below 60°C, rates of apatite annealing are very low; this temperature range is normally referred to as the total stability zone (TSZ) (Wagner 1981). Within the partial annealing zone (PAZ), rates of annealing increase dramatically until 120 ± 10°C. Above 120 ± 10°C, the annealing rates are so high that tracks are not retained and the total annealing zone (TAZ) commences. Fission tracks are formed continuously through time; if a crustal section is brought to the surface as a coherent block by uplift and erosion, apatite from the TAZ will cool and begin to record AFT ages which represent 'cooling ages'. The oldest of these ages will be closest to the timing of onset of cooling. Samples brought up from within the PAZ will record progressively younger ages with the increase of depth and attain an age similar to the cooling age at the base of PAZ. Because of significant annealing in this zone the ages have no direct relationship to geological events and are referred to as 'mixed ages' (Green *et al.* 1989). Samples from within the TSZ will record the oldest ages, reflecting the original emplacement of the host rocks or previous exhumation events.

'Mixed ages' and 'cooling ages' of apatite samples which have experienced contrasting histories can easily be distinguished by combining AFT ages with the analysis of horizontally confined track length (TL) distribution (Gleadow *et al.* 1986). Apatite samples that are exhumed from the TAZ show unimodial TL distributions; the mean TL will depend on the rate of cooling. Fast cooling is normally exemplified by long and narrowly distributed TL while short and broadly distributed tracks indicate slow uplift. TL distributions of samples

cooled from within the PAZ are positively skewed, with a progressive increase of the width of the distribution and a steady decrease of mean track length with increasing temperature (depth of burial). Apatites exhumed from near the bottom of PAZ yield broad and bimodal TL distributions consisting of a small peak or tail of short tracks which have undergone progressive shortening due to prolonged exposure to near-total annealing temperatures prior to cooling, and a pronounced peak of less annealed tracks which have accumulated during subsequent cooling (Gleadow *et al.* 1986).

Sampling procedure

Samples were collected from four profiles on the scarps of the Pangani rift at Usambara, South and North Pare mountain blocks (Fig. 1). A traverse was done from Mombo up the scarp to Soni village and then towards the Bumbuli road. Another transect was sampled from Same up the South Pare block. A third transect was done from Mwanga up the scarp to Usangi village and then down the scarp on the other side of the North Pare block towards Umba plains. A fourth transect of sampling was done on the Kilomeni scarp south of Usangi. One sample was also collected from the basement rocks cropping out within the basin floor. Dating was done using external detector methods at the fission track lab of the University of Lyon in France; details on the methodology can be found in Hurford and Green (1982) and Van der Beek (1995).

RESULTS

The ages of AFT data fall in the range of 48±4 to 207±8 Ma and are summarised in Table 1. All the fission track ages are much younger than the age of regional metamorphism. However, they predate the development of the East African Rift System. Doming within the EARS is suggested to have been initiated at around 23 Ma, during Early Miocene time (Ebinger *et al* 1989). Faulting and volcanism in the northern Tanzania sector of the rift did not start until Late Miocene, the oldest volcanic rocks known are dated at 8 Ma (Dawson 1992)

From the Usambara mountain scarp, samples EAR1 to EAR10 collected from elevations between 480 m to 1510 m ASL were analysed. On the basis of TL distribution, AFT ages from this profile can be divided into three groups. Samples EAR1 to EAR4 from altitudes of 480 to 840 m show nearly concordant AFT ages that range from 48±4 to 64 ±6 Ma. Samples from this interval yield long TL ranging from 13.6 to 14.4 μm which are narrowly distributed with a standard deviation of 1.0 to 1.3 μm. Up the Usambara scarp samples EAR5 and EAR6, from altitudes 950 m to 1050 m, the mean track lengths decrease to 12.9 to 13.4 μm, while ages increase to 75 ±5 to 81± 6 Ma. TL distributions are broader with standard deviation of 1.6 to 2.2 μm. Above 1100 m samples EAR7 to EAR10 have AFT ages ranging from 159±19 to 195±22 Ma. Mean track lengths decrease to a range of 10.3 to

10.8 μm, while their distributions become even broader with a standard deviation varying from 2.7 to 3.0 μm.

Table 1: Results of AFT analyses with sample locations and elevations. All ages are reported as central ages and calculated using the zeta callibrations approach. Samples collected from Pare and Usambara mountains, Tanzania

Sample No	Longitude (E)	Latitude (S)	Elevation (M)	Grains Counted	Ft Age (Ma)	TL μM	SD μM
EAR1	045250	381734	480	19	484	14.40.3	1.3
EAR2	045240	381750	550	20	504	13.60.1	1.3
EAR3	045310	381829	660	20	646	14.10.1	1.1
EAR4	045349	381922	840	20	605	13.80.1	1.0
EAR5	045242	382034	950	20	816	12.90.2	2.2
EAR6	045143	382108	1050	20	755	13.40.1	1.6
EAR7	045102	382157	1160	20	15919	10.80.6	2.7
EAR8	045045	382225	1280	20	18020	10.30.5	2.9
EAR9	045027	382245	1350	20	17723	10.70.5	3.0
EAR10	044955	382336	1510	20	19522	12.40.3	3.1
EAR11	040912	375055	1010	20	674	13.90.2	1.5
EAR12	040952	375151	1060	20	744	12.00.2	2.4
EAR13	040912	375214	1320	20	1579	11.50.2	2.6
EAR14	041103	373519	580	20	17610	11.30.3	2.6
EAR16	034746	373924	1090	20	625	-	-
EAR17	034803	373918	1190	20	11010	11.70.3	2.8
EAR18	034753	373947	1270	20	1598	11.90.2	2.3
EAR19	034749	374010	1350	20	17610	11.30.3	2.6
EAR20	034713	373951	1450	20	20415	10.80.3	2.2
EAR21	034624	373913	1540	20	19911	11.10.2	2.0
EAR22	033934	373558	860	20	535	-	-
EAR23	034106	373710	940	20	564	13.40.2	1.7
EAR24	034001	373736	1010	20	604	13.60.3	1.3
EAR26	033940	373800	1190	20	806	12.30.2	2.2
EAR27	034017	373826	1280	20	16212	11.30.4	2.6
EAR28	034034	373900	1320	20	1787	11.60.2	2.6
EAR29	034052	373930	1340	20	19510	11.40.2	2.2
EAR30	034328	374125	1260	20	2078	10.40.2	2.3
EAR31	034325	374158	1140	20	704	12.50.2	2.0
EAR32	034321	374207	1060	20	744	12.00.2	1.9
EAR33	034342	374229	960	20	624	13.80.2	1.6
EAR34	034346	374238	830	20U	603	14.10.2	1.2

- = not dated

Samples EAR11 and EAR13 are from the Same scarp collected from an altitude of 1010 m through to 1320 m. Based on TL distribution, samples from this profile can also be divided into the three groups described above. Sample EAR11 from an elevation of 1010 m has an AFT age of 67±4 Ma. TLs of this sample are long (13.9 μm) and are narrowly distributed with a

standard deviation (1.5 μm). Sample EAR12 from an altitude of 1060 m shows an AFT age of 74±4 Ma with relatively short (12.0 μm) and broad TL distribution having a standard deviation of 2.4 μm. Sample EAR13 from the elevation of 1320 m shows an AFT age of 157±9 Ma. The TLs of this sample are short (11.5±0.2 μm) with a broad distribution and standard deviation of 2.6 μm.

Sample EAR14 was collected west of Same town, on a basement ridge within the Pangani basin at an elevation of 580 m. This sample gives an AFT age of 176 ±10 Ma with short TL (11.3±0.3 μm) which are broadly distributed, with a standard deviation of 2.6 μm.

Samples EAR16 through to EAR21 are from the Kilomeni profile and were collected from a profile elevation of 1090 to 1540 m ASL. These samples can also be divided into three groups on the basis of TL distribution. Sample EAR16 from an elevation of 1090 m shows an AFT age of 62±5 Ma. TL distribution for this sample were not clearly defined. The next sample EAR17 collected at an elevation of 1190 m shows an AFT age of 110±10 Ma with short mean TL of 11.7±0.3 μm and broad distribution (standard deviation = 2.8 μm). Samples EAR18 through to EAR21 from an mean elevation of 1270 m and above show age range from 159±8 to 204±15 Ma. Mean TLs are short and range from 10.8 ± 0.3 to 11.9±0.2 μm. Their distribution is broad with a standard deviation of 2.0 to 2.8 μm

Samples EAR22 through to EAR34 are from the Usangi scarp profile and were collected from elevation between 860 m to 1340 m ASL. Samples EAR22 to EAR24 from the altitude of 860 to 1010 m ASL show AFT ages increasing from 53±5 Ma to 60±4 Ma. Samples from this interval yield mean TL ranging from 13.4 ±0.2 to 13.6±0.3 μm with standard deviations of 1.3 to 1.7 μm. Up the Usangi scarp, at altitude 1190 m, sample EAR26 has an AFT age of 80±6 Ma. The mean TL of this sample is 12.3 μm with a standard deviation of 2.2 μm. Samples EAR27 to EAR30 were obtained from altitudes 1190 m and above. These samples show increasing AFT ages ranging from 162±12 to 207±8 Ma. Mean TL decrease to the range of 10.4 to 11.6 μm and TL distributions are broad with standard deviations varying from 2.2 to 2.6 μm. Samples EAR31 through EAR34, collected at elevations 1040 to 830 m ASL are from the profile overlooking the Umba plains. Samples EAR31 and EAR32 (AFT ages = 70±4 to 74±4 Ma), show relatively short TL (12.0 to 12.5 μm) which are broadly distributed, with standard deviations of 1.9 to 2.0 μm. Samples EAR33 and EAR34 (AFT ages = 62±4 to 60±3 ma) give TL distributions that are long (13.8 to 14.1 μm) and narrowly distributed with standard deviations of 1.2 to 1.6 μm.

DISCUSSION

Samples EAR1 to EAR5 from the base of Usambara scarp with AFT ages ranging from 48±4 to 64±6 Ma) show relatively long TL, with a narrow range of distribution. The form of AFT length distributions indicate that rocks exposed near the base of the Usambara scarp started cooling through about 110^{0}C before around 64±6 Ma for older samples and 48±4 Ma for younger samples during Palaeocene to Eocene time. The relatively long TL distributions of these samples indicate that they spent a short interval of time within the PAZ (Gleadow *et al.* 1986). Samples EAR5 and EAR6 collected at an interval of 950 m to 1050 m show AFT ages in the range of 75±5 to 81±6 Ma. Mean TL of these samples are short (12.9 to 13.4 μm) and TL distribution are broad (1.6 to 2.2 μm) when compared to samples that have cooled rapidly (Gleadow *et al.* 1986). These AFT ages suggest that the exposed rocks cooled through the PAZ during Campanian time. The relatively short TL distribution of these samples indicate that the cooling was slow and the rocks spent a prolonged period of time within the PAZ. Samples EAR7 through to EAR10 yielded AFT ages increasing from 159±19 to 195±22 Ma with short (10.3 to 10.8 μm) and broad TL distribution, standard deviation varying from 2.7 to 3.0 μm. The short and broad TL distributions are consistent with slow cooling. The oldest sample cooled relatively slowly below 110^{0}C during Lias, while the final phase of cooling that was relatively rapid occurred at the close of Mid Jurassic.

The long and narrowly distributed TL of sample EAR11 exposed at the base of Same scarp (1010 m) suggest that rocks from the lower section of this block cooled fast through about 110°C before 67±4 Ma to around 60^{0}C during Palaeocene time. The 74 ± 4 Ma AFT age of sample EAR12 from the elevation of 1060 m, of the Same scarp, suggests that rocks from this elevation cooled through the PAZ during Campania time. The relatively short and broad TL distributions, suggest slow cooling. Rocks from 1320 m and above along the Same scarp (157±9 Ma) that show short and broad TL must have slowly cooled through the PAZ towards the end of Mid Jurassic, at the latest.

Sample EAR14 collected on a basement ridge within the Pangani basin, shows an age and TL distribution that are similar to those given by samples from the top of Pangani rift scarps. This rock sample was collected from a tectonicaly down faulted block. The short and broad TL distribution suggest slow cooling through the PAZ at about 176±10 Ma during Middle Jurassic time.

TL distribution of samples EAR16 from an elevation of 1090 m of Kilomeni profile are not clearly defined but the age of this sample fall within the range of the Early Tertiary cooling event (62±5 Ma). Mean TL of sample EAR 17 (AFT age = 110±10 Ma) at an elevation of 1190 m are short (11.7±0.3 μm) and broad (2.8 μm) suggesting that these rocks spent a prolonged period of

time within the PAZ before they were uplifted during Mid Cretaceous. Samples EAR18 through EAR21 from 1270 m and above of the Kilomeni profile (age = 159 ±8 to 204±15 Ma) have shorter (10.8±0.3 to 11.9±0.2 μm) and broader (age = 2.0 to 2.8 μm) TL distribution which are consistent with slow cooling of the area. The oldest sample from this area cooled below 110^{0}C around 204 ± 15 Ma close to the Triassic/Jurassic boundary. The final phase of cooling did not take place until Mid Jurassic at around 159 Ma.

The relatively long and narrow TL distribution of samples EAR22 to EAR24 from below 1010 m of the Usangi scarp indicate that rocks near the base of Usangi scarp underwent geologically rapid cooling from temperatures >110^{0}C to below 60^{0}C during Early Tertiary time. The oldest samples (age = 60 ± 4 Ma) cooled through the PAZ during Palaeocene, but the final phase of uplift did not take place until 53 Ma, during the Eocene. Samples EAR26 collected at an elevation of 1190 m of the Usangi scarp show an AFT age of 81 ± 6 Ma. Mean TL of this samples are short (12.3 μm) and are broadly distributed (standard deviation = 2.2 μm). The form of TL length distributions indicate that rocks exposed in this area started cooling through about 110^{0}C around 80 ± 6 Ma, during Campanian. The relatively short and broad TL distribution of these samples indicate that they spent a prolonged period of time within the PAZ. Samples EAR27 through EAR30 give AFT ages increasing from 162 ± 12 to 207 ± 8 Ma with short (10.4 to 11.6 μm) and broad (standard deviation = 2.2 to 2.6 μm) mean TL, consistent with slow cooling. The oldest sample cooled below 110^{0}C at about 207 Ma, close to the Triassic/Jurassic boundary. The final phase of cooling that was relatively rapid occurred during Mid Jurassic (62 Ma).

Samples EAR31 and EAR34 from the profile overlooking the Umba plain at an elevation of 1140 to 860 m have a similar thermal history to samples from the other side of the North Pare Block. Samples EAR31 and EAR32 (age = 70 ± 4 to 74 ± 4 Ma) show relatively short (12.0 to 12.5 μm) and broad TL distribution with standard deviation of 1.9 to 2.0 μm. The short and broad TL distributions suggest slow cooling during Campanian time. Samples EAR33 and EAR34 (age = 62 ± 4 to 60 ± 3 Ma) give TL distributions that are long 13.8 to 14.1 μm and narrowly distributed, with standard deviations of 1.2 to 1.6 μm. Uplift of these samples must have taken place fast during Palaeocene.

CONCLUSION

The current AFT data suggest that topographic patterns exposed on the flanks of the Pare-Usambara mountains represent surfaces that are products of three phases of tectonic uplift: Early Jurassic, Late Cretaceous and Early Tertiary time. Erosion and isostatic rebound have modified the tectonically induced topographic patterns and samples from the upper part of the scarps show a surface which is a remnant of Karoo uplift event corresponding to the

'Gondwana surfaces' of eastern Africa eroded slowly since Precambrian time. The short and broad TL distribution of these samples are consistent with slow cooling of the area after the peak of the Pan African thermal event about 550 Ma (Kennedy 1964). The Pan African thermal event is the last thermal event recorded within the Mozambique belt. 'Gondwana surfaces' in eastern Africa stand high between 1500 - 3000 m ASL level and are occupied by core stoned bedrock implying overprinting of a number of erosional cycles (Mutakyahwa 1992).

Sediments within the Pangani basin are relatively thin and not well studied, however, the three tectonic events described above can be easily reflected in the sedimentary record of the Tanzania coastal basin, of which the Pare-Usambara mountains have been major suppliers of sediments. The first phase of significant uplift seems to have been initiated at the Early part of Jurassic, during Lias. This probably can be equated to the last Karoo tectonic event, the Triassic/Early Jurassic tectonic event of Wopfner (1990). Karoo sedimentation in coastal Tanzania is recorded to have been terminated by a number of tectonic pulses: seismic interpretation indicate that significant thickness of Triassic and earlier sediments must have been removed by the Pre to Early Jurassic erosion (Mbede & Dualeh 1997). The youngest Karoo sediments in coastal Tanzania are refereed to as Ngerengere beds and are dated as Early Jurassic (Kent *et al.* 1971, Balduzz *et al.* 1992). Ngerengere beds are made up of complex sequences separated by disconformities indicating different cycles of deposition in response to tectonic control of the bounding faults. The basal sequence of these beds are made up of conglomeratic material that reflect uplift of the sediment source areas. On the overall, Mid to Late Cretaceous in coastal Tanzania is recorded to be transgressive. However, a basal conglomerate recorded at the Senonian/Campanian boundary indicates uplift of the source areas during the time at least locally. Though still deep marine sediments are recorded almost everywhere in Palaeocene, the gas show in Zanzibar 1, Pemba 5 and Mafia 1 are reported in Palaeocene sands (Kajato 1982). These sediments indicate shallowing of the sea resulting from a regressive phase that is more recognized in Eocene and continued into Oligocene along coastal Tanzania (Kent *et al.* 1971, Kent & Pyre 1973).

ACKNOWLEDGEMENT

This work was partially financed by the faculty support of the Sida/SAREC project. Fission track dating was facilitated through a generous support of the University of Lyon fission track laboratory in France.

REFERENCES

Anon 1980 *Internal report for feasibility study on lower Moshi agricultural project.* JICA; Nipon koei Co. Ltd. Pasco International Inc.

Bagnall PS 1962 North Pare Quarter degree sheet 73. *Tang. Geol. Surv. Map*

Bagnall PS, Dundas D and Hartley EW 1963 Lushoto Quarter degree sheet 109. *Tang. Geol. Surv. Map*

Balduzz A, Msaky E Trincianti E and Manum SB 1992 Mesozoic Karoo and post-Karoo formations in the Kilwa area, southern Tanzania - a stratigraphic study based on palynological, micropaleontology and well log data from Kizimbani. *J. Afr. Earth Sc.* 3/4: 405-427

Dawson JB 1992 Neogene tectonics and volcanicity in northern Tanzania sector of the Gregory rift valley: constraints with the Kenya rift sector. *Tectonophys. 204:* 81-92

Ebinger CJ Bechtel TD Forsyth DW and Bowin CO 1989 Effective elastic plate thickness beneath the East Africa and Afar Plateaus and dynamic compensation for the uplifts. *J. Geophys. Res 94/83:* 2883-2901

Ebinger CJ Poudjom Y, Mbede EI and Foster A 1996 Rifting Archean lithosphere: the Eyasi-Natron-Manyara rifts, East Africa. *J. Geol. Soc. 154:* 947-960

Fairhead JD, Watts AB, Chevalier P, El-Haddedeh B, Green CM, Stuart GW, Whaler KA and Windle I 1988 *Africa gravity project,. Commercial report* University of Leeds, Leeds, UK

Gleadow AJW, Duddy IR, Green PF and Hegarty KA 1986 Fission track lengths in the apatite annealing zone and the interpretation of mixed ages. *Earth Planet. Sci. Lett.* 78: 245-254

Green PF, Duddy IR, Gleadow AJW and Lovering JF 1989 Apatite fission track analysis as a paleotemperature indicator for hydrocarbon exploration.- In: Naeser ND and McCulloh TH (eds) *Thermal histories of sedimentary basins: methods and case histories.* pp 181-195

Hurford TP and Green PF 1982 A users' guide to fission track dating calibration. *Earth Planet. Sci. Lett. 59: 343-354*

Ilangali NM 1988 Geologic and economic aspects of some non-metallic minerals in Tanzania: Limestone, Gypsum, Silica Sand, Pegmatite, Feldspar, Quartz and Nepheline Syenite. In: Kimambo RH (ed) *Development of the non-metallic minerals and the Silicate industry in Tanzania.* East African Publications Ltd. pp 21-79

Kajato HK 1982 Gas strike spur: search for oil in Tanzania. *Oil and Gas journal.* March: 123-130

Kennedy WQ 1964 The structural differentiation of Africa (500 my) tectonic episode. *Ann Rep. Res. Inst. African Geol.* (Univ. Leeds) 8*:* 48-49

Kent PE and Pyre JTO 1973 The development of Indian Ocean margin in Tanzania In: Blant G (eds) *Sedimentary basins of African coasts part 2: South and East coasts.* Paris Assoc. des services Geol. Africans pp 113-131

Kent PE, Hunt JA and Johnstone DW 1971 *The geology and geophysics of coastal Tanzania.* Geol. Sci. London Inst. Geophys. Sc. Geophysics paper 6

Mbede EI 1999 The structure of Pangani Rift Basin from Geophysical data. In: Logatchev NA, Levi K, Sankov V and Rasskazov S (eds) *Rifting in continental setting: Baikal Rift system and other Rifts Irkutsk and Lake Baikal:* pp 22-30

Mbede EI and Dualeh A 1997 The coastal basins of Somalia, Kenya and Tanzania. In:Selley RC (eds) *African basins. Sedimentary Basins of the World 3.* Elsevier Science B.V pp 211-233

McConnell RB 1972 Geological development of the rift system of eastern Africa. *Bull. Geol. Soc. Amer. 83* 2549-2572

Mutakyahwa MKD 1991 *Mineralogy, geochemistry and genesis of laterites and bauxite on the Precambrian basement of Eastern Tanzania, East Africa.* Dissertation Hamburg

Nyblade AA, Birt C, Langston C, Owens T and Last R 1997 Seismic experiment probes cratonic structure beneath East Africa and reveals locus of rifting in NE Tanzania. *Eos Trans. Amer. Geophys. Union* 77: 563-587

Upcott NM, Mukasa RK, Ebinger CJ and Karner GD 1996 Along-axis segmentation and isostasy in the northern Western rift, Africa. *J.Geophys. Res.* 101: 3247-3268

Van der Beek P 1995 *Tectonic evolution of continental rifts: inference from numerical modelling and fission track thermalchronology.* PhD thesis, Free Univ. Amsterdam

Wagner GA 1981 Fission track ages and their geological interpretation. *Nucl. Tracks 5* (1/2): 15-25

Wopfner H 1990 *Rifting in Tanzania Karoo basins and its economic implications.* 15th Colloquium of African Geology. Centre Internat. pour la Formation et les Exchanges Géologiques Occ. Pub. 20 pp217-220